mathematics

Article

Eigenvalue Problem Describing Magnetorotational Instability in Outer Regions of Galaxies

Evgeny Mikhailov [1,2,3,*] and Tatiana Khasaeva [1,4]

1 Faculty of Physics, M. V. Lomonosov Moscow State University, 119991 Moscow, Russia
2 P. N. Lebedev Physical Institute, 119991 Moscow, Russia
3 Center for Advanced Studies, Skolkovo Institute of Science and Technology, 121205 Moscow, Russia
4 Institute of Earthquake Prediction Theory and Mathematical Geophysics, 117997 Moscow, Russia
* Correspondence: ea.mikhajlov@physics.msu.ru

Abstract: The existence of magnetic fields in spiral galaxies is beyond doubt and is confirmed by both observational data and theoretical models. Their generation occurs due to the dynamo mechanism action associated with the properties of turbulence. Most studies consider magnetic fields at moderate distances to the center of the disk, since the dynamo number is small in the marginal regions, and the field growth should be suppressed. At the same time, the computational results demonstrate the possibility of magnetic field penetration into the marginal regions of galaxies. In addition to the action of the dynamo, magnetorotational instability (MRI) can serve as one of the mechanisms of the field occurrence. This research is devoted to the investigation of MRI impact on galactic magnetic field generation and solving the occurring eigenvalue problems. The problems are formulated assuming that the perturbations may possibly increase. In the present work, we consider the eigenvalue problem, picturing the main field characteristics in the case of MRI occurrence, where the eigenvalues are firmly connected with the average vertical scale of the galaxy, to find out whether MRI takes place in the outer regions of the galaxy. The eigenvalue problem cannot be solved exactly; thus, it is solved using the methods of the perturbation theory for self-adjoint operators, where the eigenvalues are found using the series with elements including parameters characterizing the properties of the interstellar medium. We obtain linear and, as this is not enough, quadratic approximations and compare them with the numerical results. It is shown that they give a proper precision. We have compared the approximation results with those from numerical calculations and they were relatively close for the biggest eigenvalue.

Keywords: eigenvalue problem; magnetorotational instability; perturbation theory; operator

MSC: 76W05; 47A75

check for updates

Citation: Mikhailov, E.; Khasaeva, T. Eigenvalue Problem Describing Magnetorotational Instability in Outer Regions of Galaxies. *Mathematics* **2024**, *12*, 760. https://doi.org/10.3390/math12050760

Academic Editor: Zhoujian Cao

Received: 7 February 2024
Revised: 27 February 2024
Accepted: 2 March 2024
Published: 4 March 2024

1. Introduction

It is well known that a large variety of astrophysical objects, such as the Sun [1,2], the Earth [3], other planets [4,5] and stars [6–8], accretion discs [9,10], pulsars [11] and some galaxies [12,13], have large-scale magnetic fields. There are different methods of observational study for such fields. For example, for the Sun, we can use the Zeeman effect [14]. As for faraway objects (galaxies and accretion discs), this approach cannot give any proper results, so it is necessary to study the synchrotron emission spectra [15]. Nowadays, for most cases, Faraday rotation measurements are taken [16,17]. This method is based on the fact that the polarized radio wave (passing, for example, from pulsars) changes its polarization plane angle while travelling through a magnetized medium. The angle of rotation is proportional to the integral of magnetic field projection to the line of sight. Also, it depends on the wavelength, being proportional to its square. Thus, comparing polarization angles for different wavelengths, we can rebuild the field structure.

Observations give the typical value of the field of order of microgauss for galaxies [18]. As for the accretion discs, magnetic field studies are much more difficult. They are connected with the small size of such objects, especially for ones situated near white dwarfs, neutron stars and black holes with masses comparable to the Sun. They cannot be studied because of the poor resolution, even for most modern instruments. The problem is slightly easier for the accretion discs of the supermassive black holes situated in the central parts of galaxies. However, even for this case, there is only one example of effective Faraday rotation measurements in the nuclei of M87, but all the conclusions about the field structure are still being discussed [19,20].

From a theoretical point of view, there are several approaches to explain the magnetic field generation. One of the most important processes is connected with the dynamo mechanism. It can be divided into two different scales [21]. The first one is based on local vorticed turbulent motions and can cause the occurrence of only a random small-scale field. The large-scale magnetic dynamo is much more important. It is based on the differential rotation (most of the astrophysical objects rotate in non-solid mode) and the helicity of the turbulent motions. The law for the field can be obtained by averaging the classical magnetohydrodynamics equations. The growth of the field can be restricted by the turbulent diffusivity destroying the large-scale structures. It leads us to the idea that the magnetic field growth is a threshold process. Mathematically, the diffusivity is connected with dissipation terms in the equations. If we discuss whether the field can grow, we should solve the parabolic equation. The properties of the equation give us an opportunity to assume that the field growth is exponential, and we can reduce the problem to an eigenvalue problem [22,23], where the eigenvalues mean the field growth rates and the eigenfunctions describe its spatial structure. There are several works [23,24] where critical values of the parameters corresponding to the field growth (or its decay) are obtained. This approach allows us to describe the magnetic field in some galactic objects and (for some cases) in the accretion discs.

The large-scale dynamo properly works for the main parts of the astrophysical discs (as for the galaxies, it is limited by 8–10 kpc). However, if we consider the field for larger distances from the center of the object, the dynamo is much weaker than in the inner parts. Previously, it has been shown that the dynamo number characterizing the efficiency of the main processes is generally lower than the critical one, so that the field cannot be generated. Though the situation may be partly mitigated by assuming the non-linear effects occurrence, the dynamo still cannot generate significant magnetic fields in the outer parts of the galactic or accretion discs [25]. Nevertheless, there are certain physical reasons for the fields in the outer parts to exist.

However, there are other mechanisms that can explain the occurrence of magnetic fields in cosmic discs, especially in their outer parts. We should mention the mechanism, which is discussed in some of the classic works. It is connected with magnetorotational instability and explains the transition of both the magnetic field and angular momentum in the radial direction [26–32]. The possibility of such a process in accretion discs was described in detail in a recent work by Shakura and coauthors [33]. This research comprises not only the investigation of physical processes but also the mathematical study of the problem, comprising both analytical and numerical considerations of occurring problems.

This approach can also be used to describe the field generation in the outer parts of the galaxies. Though some physical processes in galactic and accretion discs have much in common (taking the size difference into account), it is necessary to add some changes into the model associated with the galaxies [9]. In particular, it is especially important to take into account some distinctions in rotational laws. The accretion discs' rotation can be described by Kepler law [34]. In the case of galaxies, we simply use either the flat rotational curve or, for more accurate description, the Brandt rotational curve [35,36].

We obtain the magnetic field equation by transforming magnetohydrodynamics equations with some approximations. We shall use the model, according to which the magnetic field and velocity components are described by the harmonic law [33]. In this case, the equation can be turned into an eigenvalue problem. To describe the possibility of magnetic field generation, we have to study its eldest spatial mode. Taking the time dependence, we are going to use the harmonic law as well. The growth of the magnetic field is connected with the transition of its oscillation frequency from real range to imaginary. Thus, it is possible to reconstruct the previous problem into the study of the eldest eigenvalue which characterizes the vertical scaleheight.

Despite the apparent simplicity, calculating the eigenvalues and eigenfunctions appeared to be challenging. Finding their exact meanings seems to be impossible; we can find them approximately using the fact that linear operators are self-adjoint. This allows us to use the perturbation theory, which has been developed for the operators in quantum mechanics [37]. The problem specialties in some cases do not give us any opportunity to use only the first order of the perturbation theory. For this reason, we have to consider the second order as well. A numerical solution of such problems also appears to be challenging.

This paper is organized in the following way. Firstly, we formulate our model and obtain the main equations. After that, we find the eigenvalues for the flat rotational curve, taking perturbation theory methods into account. We then pass to a more difficult case, connected with the Brandt rotational curve, where we also use perturbation theory methods. We also describe numerical solutions for both cases. Finally, we discuss the results and their astrophysical applications.

2. Basic Equations

Magnetic field generation in the outer parts of the galactic discs can be connected with magnetorotational instability, which is widely known in different problems in hydrodynamics. Firstly, for the equilibrium case, the rotating fluid is moving under the pressure gradient and the centrifugal force that counterbalance each other. If the outer parts of the fluid move with smaller angular velocity, instability can develop, and the angular momentum will pass in the radial direction. However, it is necessary to have quite a large angular velocity gradient: according to the Rayleigh criteria [26], it should decrease faster than $\frac{1}{r^2}$.

The situation principally changes for magnetohydrodynamical problems, if the fluid has a frozen-in magnetic field. In this case, instability will be developed even for small gradients of the angular velocity. For this case, the magnetic field can pass from the inner parts of the rotating object to its outer ones.

The possibility of magnetorotational instability existence is connected with the plasma parameter [28], which describes the ratio between the hydrodynamic pressure and the magnetic one:

$$\beta = \frac{8\pi P}{B_0^2}, \tag{1}$$

where P is the hydrodynamic pressure and B_0 is the magnetic field induction. The process can work if $\beta >> 1$. In the case of the outer parts of the galaxies, we can estimate the pressure by the order of 10^{-12} dyn cm^{-2}. As for the initial magnetic field (B_0), which can be connected with relatively weak dynamo action, it can be estimated as 10^{-7} G [25]. So, the plasma parameter will be $\beta \sim 10^3$, which is quite sufficient for magnetorotational instability. Thus, we state that MRI can occur in galaxies.

As for the mathematical formulation of the problem, we use methods which are similar to ones described in [33]. We assume that the field and velocity fluctuations are proportional to the cosine $\cos(\omega t - k_z z)$, where ω relates to the circular frequency and k_z characterizes the inverse lengthscale in the vertical direction.

If we transform the equations for the field (induction equation) and the velocity (Euler equation), we obtain the equation for B_r. However, it is not very convenient because of the first r-derivative which will make some of the operators become non-self-adjoint. Thus, to simplify the problem, the function $\psi(r) = B_r(r)\sqrt{r}$. was taken, where $B_r(r)$ is the radial magnetic field considered in cylinder coordinates.

The following equation can be obtained [33] from the Navier–Stokes equation and the magnetic field evolution equation in magnetohydrodynamics:

$$\frac{d^2\psi}{dr^2} + \left[-\frac{3}{4r^2} + \frac{\omega^2}{k_z^2} \frac{2\Omega\left(2\Omega + r\frac{d\Omega}{dr}\right)}{\left(c_0^2 - \frac{\omega^2}{k_z^2}\right)^2} - \frac{2\Omega c_0^2 r \frac{d\Omega}{dr}}{\left(c_0^2 - \frac{\omega^2}{k_z^2}\right)^2} \right] \psi = k_z^2 \psi; \tag{2}$$

where $c_0 = \frac{B_0}{2\sqrt{\pi\rho}}$ is the Alfven velocity and Ω is the angular velocity of the disc.

We are interested in the borderline case between the oscillating solution (the frequency is real and $\omega^2 > 0$) and the exponentially growing one. For this regime, we have the exponential growth rate γ and the imaginary "frequency" $\omega = i\gamma$ and $\omega^2 < 0$. In this case, we take $\omega = 0$. Equation (2) transforms into:

$$\frac{d^2\psi}{dr^2} + \left[-\frac{3}{4r^2} - 2\Omega c_0^{-2} r \frac{d\Omega}{dr} \right] \psi = k_z^2 \psi; \tag{3}$$

For the simplest case, we take the flat rotation curve. We note that in the case of galaxies, in contradistinction to accretion discs, where the Kepler rotation curve is used [34], it is reasonable to use constant linear velocity as the first approximation base. It is known that for large distances from the center, the linear velocity of the galaxy is nearly constant ($V = V_0$). So, the angular velocity will be $\Omega(r) = \frac{V_0}{r}$. Equation (3) will become:

$$\frac{d^2\psi}{dr^2} + \left[-\frac{3}{4r^2} + \frac{2V_0^2}{c_0^2 r^2} \right] \psi = k_z^2 \psi; \tag{4}$$

Measuring the distances in the radius of the main part of the galaxy, we obtain the following eigenvalue problem:

$$\lambda\psi = \frac{d^2\psi}{dr^2} + \frac{C}{r^2}\psi; \tag{5}$$

with boundary conditions (here, we assume that the field becomes zero at two radiuses of the main part):

$$\psi|_{r=r_{\min}} = \psi|_{r=r_{\max}} = 0. \tag{6}$$

Here, we have introduced $C = \frac{2V_0^2}{c_0^2} - \frac{3}{4}$.

In the case of a more accurate model for the galaxy rotation, we use the Brandt rotation law [35]:

$$\Omega(r) = \frac{\Omega_0}{\sqrt{1 + \frac{r^2}{r_0^2}}} \tag{7}$$

where Ω_0 is the typical angular velocity and r_0 is the lengthscale of its changing. The Brandt rotation law is a good approximation which corresponds to observational data and it comprises simplicity and proper accuracy, while more complicated laws are discussed in [36–38]. As for large r, the Brandt rotation law transforms into a simpler plane rotation curve:

$$\Omega(r) = \frac{V_0}{r} + O\left(\frac{1}{r}\right); \tag{8}$$

The equation will be:

$$\frac{d^2\psi}{dr^2} + \left[-\frac{3}{4r^2} + \frac{2r_0^2 r^2}{c_0^2} \frac{\Omega_0^2}{(r_0^2 + r^2)^2} \right] \psi = k_z^2 \psi; \tag{9}$$

It corresponds to an eigenvalue problem:

$$\lambda\psi = \frac{d^2\psi}{dr^2} - \frac{3}{4r^2}\psi + \frac{Dr^2}{\left(r_0^2 + r^2\right)^2}\psi. \tag{10}$$

with boundary conditions (6).

3. Eigenvalue Problem for Flat Rotation Curve

Firstly, we need to solve the eigenvalue problem:

$$\lambda\psi = \hat{H}\psi + \hat{V}\psi; \tag{11}$$

where $\hat{H} = \frac{d^2}{dr^2}$ and $\hat{V} = \frac{C}{r^2}$ with boundary conditions (6). The non-perturbed eigenvalue can be obtained by solving the problem:

$$\lambda^{(0)}\psi = \hat{H}\psi; \tag{12}$$

Thus, non-perturbed eigenvalues can be found from the following expression:

$$\lambda_n^{(0)} = -\frac{\pi^2 n^2}{\left(r_{\max} - r_{\min}\right)^2}; \tag{13}$$

The eigenfunctions in the non-perturbed case can be easily obtained:

$$\psi_n^{(0)} = \frac{\sqrt{2}}{\sqrt{\left(r_{\max} - r_{\min}\right)}} \sin\left(\frac{\pi n(r - r_{\min})}{r_{\max} - r_{\min}}\right); \tag{14}$$

To find the perturbations for eigenvalues in the first approximation, we use the equation [39]:

$$\delta\lambda_n^{(1)} = (\psi_n, \hat{V}\psi_n); \tag{15}$$

The perturbations in our case can be found analytically by solving the integral:

$$\delta\lambda_n^{(1)} = \int\limits_{r_{\min}}^{r_{\max}} \frac{\sqrt{2}}{\sqrt{\left(r_{\max} - r_{\min}\right)}} \sin^2\left(\frac{\pi n(r - r_{\min})}{r_{\max} - r_{\min}}\right)\frac{C}{r^2}dr; \tag{16}$$

The integral in (15) can be described using the following expression:

$$\delta\lambda_n^{(1)} = C\frac{\pi n\sqrt{2}}{\left(r_{\max} - r_{\min}\right)^{3/2}}\left(\mathrm{Si}\left(\frac{2\pi n r_{\max}}{r_{\max} - r_{\min}}\right)\cos\left(\frac{2\pi n r_{\min}}{r_{\max} - r_{\min}}\right) - \mathrm{Ci}\left(\frac{2\pi n r_{\max}}{r_{\max} - r_{\min}}\right)\sin\left(\frac{2\pi n r_{\min}}{r_{\max} - r_{\min}}\right) - \right. \tag{17}$$

$$\left. -\mathrm{Si}\left(\frac{2\pi n r_{\min}}{r_{\max} - r_{\min}}\right)\cos\left(\frac{2\pi n r_{\min}}{r_{\max} - r_{\min}}\right) + \mathrm{Ci}\left(\frac{2\pi n r_{\min}}{r_{\max} - r_{\min}}\right)\sin\left(\frac{2\pi n r_{\min}}{r_{\max} - r_{\min}}\right)\right)$$

Here, $\mathrm{Si}(r) = \int\limits_0^r \frac{\sin(t)}{t}dt$ and $\mathrm{Ci}(r) = -\int\limits_r^\infty \frac{\cos(t)}{t}dt$ are integral sine and cosine functions and C is the constant value, introduced in Equation (5), which is determined by the main characteristics of the field. For some certain boundary conditions (for example, $r_{\min} = 0.5$ and $r_{\max}$ = 1.5), it can be simplified:

$$\delta\lambda_n^{(1)} = (-1)^n\sqrt{2}C\pi n(\mathrm{Si}(3\pi n) - \mathrm{Si}(\pi n)); \tag{18}$$

The first approximation is quite enough to estimate the eigenvalues in a variety of applied problems, connected with magnetic field generation in the outer regions of the galaxies. Nevertheless, there are a few examples of cases where the linear approximation is not sufficient. It is especially significant for the eldest eigenvalue, which describes the principle behavior of the magnetic field in galaxies.

To calculate the perturbations for the eigenvalues in the second approximation, we use the equation [39]:

$$\delta\lambda_n^{(2)} = \sum_{n\neq m} \frac{(\psi_n, \hat{V}\psi_m)^2}{\lambda_n^{(0)} - \lambda_m^{(0)}}; \tag{19}$$

which can be determined using expression (15):

$$\delta\lambda_n^{(2)} = \sum_{n\neq m} \frac{\left(\int\limits_{r_{\min}}^{r_{\max}} \frac{\sqrt{2}}{\sqrt{(r_{\max}-r_{\min})}} \sin\left(\frac{\pi n(r-r_{\min})}{r_{\max}-r_{\min}}\right) \sin\left(\frac{\pi m(r-r_{\min})}{r_{\max}-r_{\min}}\right) \frac{C}{r^2} dr\right)^2}{\lambda_n^{(0)} - \lambda_m^{(0)}}; \tag{20}$$

Finally, we find the eigenvalues by summing the obtained approximations for the perturbations and the non-perturbed eigenvalues, given in (13):

$$\lambda_n = \lambda_n^{(0)} + \delta\lambda_n^{(1)} + \delta\lambda_n^{(2)} + \ldots; \tag{21}$$

The approximate analytical results for several pairs of $r_{\min}$ and $r_{\max}$ (here, we confine ourselves using the first approximation) are presented in Table 1. We show linear and quadratic terms and approximate values in Table 2.

Table 1. Perturbations for the first three eigenvalues in the first approximation for eigenvalue problem (11).

	$\mathbf{r_{min} = 0.5}$ $\mathbf{r_{max} = 1.5}$	$\mathbf{r_{min} = 1}$ $\mathbf{r_{max} = 2}$
$\delta\lambda_1^{(1)}$	$1.1131 \times \mathrm{C}$	$0.4650 \times \mathrm{C}$
$\delta\lambda_2^{(1)}$	$1.2551 \times \mathrm{C}$	$0.4896 \times \mathrm{C}$
$\delta\lambda_3^{(1)}$	$1.2946 \times \mathrm{C}$	$0.4953 \times \mathrm{C}$

Table 2. Perturbations for the eldest eigenvalues and approximate meanings for eigenvalue problem (11).

	$\mathbf{r_{min} = 0.5}$ $\mathbf{r_{max} = 1.5}$	$\mathbf{r_{min} = 1}$ $\mathbf{r_{max} = 2}$
$\delta\lambda_1^{(1)}$	$1.1131 \times C$	$0.4650 \times C$
$\delta\lambda_1^{(2)}$	$0.0063 \times C^2$	$0.0004 \times C^2$
$\lambda_1(C = 600)$	2955.56	431.456

The same problem can also be solved numerically [40]. Here, we have to solve the eigenvalue problem:

$$\lambda\psi = \hat{L}_1\psi; \tag{22}$$

where $\hat{L}_1 = \frac{d^2}{dr^2} + \frac{C}{r^2}$. We will consider the function $\phi(r,t) = \sum\limits_{n=1}^{\infty} \psi_n(r)e^{\lambda_n t}$. Thus, the problem can be formulated in another way:

$$\hat{L}_1\phi = \frac{\partial\phi}{\partial t} \tag{23}$$

Taking into account that $\lambda_1 > \lambda_2 > \lambda_{n>2}$ for large values of the variable t, we conclude that:

$$\phi = \psi_1(r)e^{\lambda_1 t}(1 + O(e^{-(\lambda_1-\lambda_2)t})) \tag{24}$$

For the derivative, we obtain:

$$\frac{\partial \phi}{\partial t} = \lambda_1 \psi_1(r) e^{\lambda_1 t}(1 + O(e^{-(\lambda_1 - \lambda_2)t})) \tag{25}$$

This assumption gives us an opportunity to use the expression [23]:

$$\lambda_1 \phi \cong \frac{\partial \phi}{\partial t}; \tag{26}$$

which will lead us to the Cauchy problem:

$$\frac{\partial^2 \phi}{\partial r^2} + \frac{C}{r^2}\phi = \frac{\partial \phi}{\partial t}; \tag{27}$$

$$\phi|_{r=r_{\min}} = \phi|_{r=r_{\max}} = 0; \tag{28}$$

$$\phi|_{t=0} = 0. \tag{29}$$

The first eigenfunction is presented in Figure 1. Using the dependence (22), we can find the first eigenvalue:

$$\lambda_1 = \frac{\partial \phi}{\partial t} \cdot \frac{1}{\phi}; \tag{30}$$

The results compared to analytical values, given in Table 1, are presented in Table 3 for $r_{\min} = 0.5$, $r_{\max} = 1.5$.

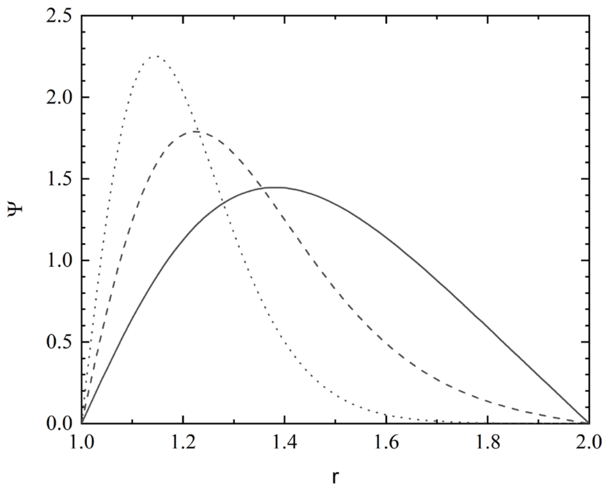

Figure 1. Dependence of ψ on distance to the center at different values of D: D = 600—dotted, D = 200—dashed, D = 50—solid.

Table 3. Analytical and numerical results comparison for eigenvalue problem (11).

C	Analytical Result for k_z	Numerical Result for k_z	Δk_z
600	20.772	19.458	1.314
400	15.756	15.338	0.418
200	10.058	10.059	0.001
100	6.414	6.415	0.001
50	3.809	3.795	0.014

4. Eigenvalue Problem for the Brandt Rotation Curve

We will then consider the problem:

$$\lambda \psi = \hat{H}\psi + \hat{L}\psi; \tag{31}$$

where $\hat{L} = -\frac{3}{4} \cdot \frac{1}{r^2} + \frac{Dr^2}{(r_0^2 - r^2)^2}$, which corresponds to the Brandt rotational curve case.

We can find the perturbations in the first approximation using Equation (15). In this case, we have to solve the integral:

$$\delta\lambda_n^{(1)} = \int_{r_{\min}}^{r_{\max}} \frac{\sqrt{2}}{\sqrt{(r_{\max} - r_{\min})}} \sin^2\left(\frac{\pi n(r - r_{\min})}{r_{\max} - r_{\min}}\right)\left(-\frac{3}{4} \cdot \frac{1}{r^2} + \frac{Dr^2}{(r_0^2 - r^2)^2}\right)dr \quad (32)$$

To simplify the expression for Equation (28), we will use the function $\tau(r)$:

$$\tau(r) = \frac{1}{8}(-1)^n[\mathrm{Ci}(2\pi n(r_0 - r)) - \mathrm{Ci}(2\pi n(r_0 + r)) + 2\pi n\mathrm{Si}(2\pi n(r_0 - r)) - 2\pi n\mathrm{Si}(2\pi n(r_0 - r))] - \quad (33)$$

$$-\frac{(-1)^{\mathrm{n}} r\cos(2\pi nr)}{4(r^2 - r_0^2)} - \frac{r}{2(r_0^2 - r^2)} - \frac{1}{2r_0 \tanh\left(\frac{r}{r_0}\right)};$$

and expression (17), obtained in the previous paragraph, which we set as $\xi(r_{\min}, r_{\max})$:

$$\xi(r_{\min}, r_{\max}) = \frac{\pi n\sqrt{2}}{(r_{\max} - r_{\min})^{3/2}}\left(\mathrm{Si}\left(\frac{2\pi n r_{\max}}{r_{\max} - r_{\min}}\right)\cos\left(\frac{2\pi n r_{\min}}{r_{\max} - r_{\min}}\right) - \mathrm{Ci}\left(\frac{2\pi n r_{\max}}{r_{\max} - r_{\min}}\right)\sin\left(\frac{2\pi n r_{\min}}{r_{\max} - r_{\min}}\right) - \quad (34)$$

$$-\mathrm{Si}\left(\frac{2\pi n r_{\min}}{r_{\max} - r_{\min}}\right)\cos\left(\frac{2\pi n r_{\min}}{r_{\max} - r_{\min}}\right) + \mathrm{Ci}\left(\frac{2\pi n r_{\min}}{r_{\max} - r_{\min}}\right)\sin\left(\frac{2\pi n r_{\min}}{r_{\max} - r_{\min}}\right)\right);$$

The calculations lead us to the expression:

$$\delta\lambda_n^{(1)} = D\sqrt{2}(\tau(r_{\max}) - \tau(r_{\min})) - \frac{3}{4}\xi(r_{\min}, r_{\max}) \quad (35)$$

The results for the perturbations in the first approximation are presented in Table 4.

Table 4. Perturbations for the eldest eigenvalues in the first approximation for eigenvalue problem (31).

	$\mathbf{r_{min}}$ **= 0.5** $\mathbf{r_{max}}$ **= 1.5**	$\mathbf{r_{min}}$ **= 1** $\mathbf{r_{max}}$ **= 2**
$\delta\lambda_1^{(1)}$	1.2408 × D − 0.8349	0.4840 × D − 0.3487
$\delta\lambda_2^{(1)}$	1.4417 × D − 0.9414	0.5121 × D − 0.3673
$\delta\lambda_3^{(1)}$	1.5051 × D − 0.9710	0.5187 × D − 0.3714

To calculate the perturbations in the second approximation, we use Equation (19), which in this case can be expressed as:

$$\delta\lambda_n^{(2)} = \sum_{n\neq m} \frac{\left(\int_{r_{\min}}^{r_{\max}} \frac{\sqrt{2}}{\sqrt{(r_{\max} - r_{\min})}} \sin\left(\frac{\pi n(r - r_{\min})}{r_{\max} - r_{\min}}\right)\sin\left(\frac{\pi m(r - r_{\min})}{r_{\max} - r_{\min}}\right)\left(-\frac{3}{4r^2} + \frac{Dr^2}{(r_0^2 - r^2)^2}\right)dr\right)^2}{\lambda_n^{(0)} - \lambda_m^{(0)}}; \quad (36)$$

The results including the second approximations for the perturbations of the eldest eigenvalues in the case of several pairs of $r_{\min}$ and $r_{\max}$ are presented in Table 5.

Table 5. Perturbations for the eldest eigenvalues and approximate meanings for eigenvalue problem (31).

	$\mathbf{r_{min} = 0.5}$ $\mathbf{r_{max} = 1.5}$	$\mathbf{r_{min} = 1}$ $\mathbf{r_{max} = 2}$
$\delta\lambda_1^{(1)}(D = 100)$	123.246	48.054
$\delta\lambda_1^{(2)}(D = 100)$	98.150	5.225
$\lambda_1(D = 100)$	211.526	43.410

Finally, to calculate the eigenvalues numerically, we use the same approach as in the previous paragraph. Using the assumption (25), we come across the Cauchy problem:

$$\frac{\partial^2 \phi}{\partial r^2} + \left(-\frac{3}{4} \cdot \frac{1}{r^2} + \frac{Dr^2}{\left(r_0^2 - r^2\right)^2}\right)\phi = \frac{\partial \phi}{\partial t}; \tag{37}$$

$$\phi|_{r=r_{\min}} = \phi|_{r=r_{\max}} = 0; \tag{38}$$

$$\phi|_{t=0} = 0. \tag{39}$$

The eigenvalues obtained due to this approach are presented in Table 6 and the eldest eigenfunctions corresponding to several values of the D coefficient are pictured in Figure 2.

Table 6. Analytical and numerical results comparison for eigenvalue problem (31).

D	Numerical Result for $\mathbf{k_z}$	Analytical Result for $\mathbf{k_z}$	$\mathbf{\Delta k_z}$
600	20.145	21.691	0.546
400	15.863	16.367	0.504
200	10.379	10.375	0.004
100	6.595	6.589	0.006
50	3.895	3.907	0.012

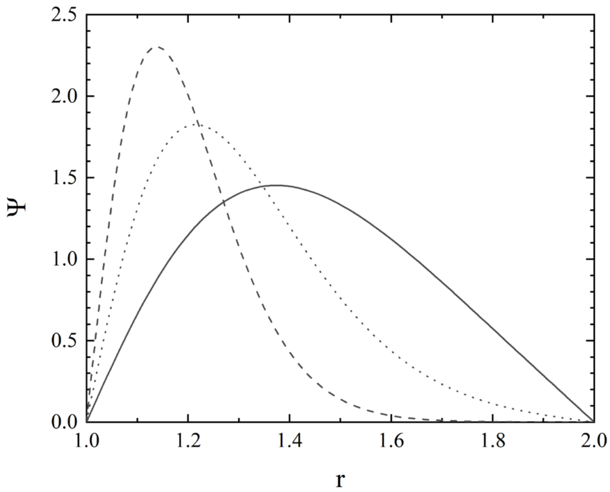

Figure 2. Dependence of ψ on distance to the center at different values of D: D = 600—dashed, D = 200—dotted, D = 50—solid.

5. Conclusions

We studied the possibility of magnetic field generation in the outer parts of galaxies due to magnetorotational instability. This process is associated with an eigenvalue problem which can be solved using perturbation theory methods. We used the approaches that are widely known in quantum mechanics. As for the linear term, the results can be obtained purely analytically, while in the case of the quadratic one, it is necessary to calculate the integrals numerically. It would be interesting to also study further approximations, but the comparison with numerical studies shows that they are not likely to make any significant changes. After comparing the numerical results and the analytical approximations, we note that the difference is more significant for large values of C. This may be due to the fact that the approximation results are based on perturbation theory methods, which assume that the perturbations proportional to C are relatively small. The larger C is, the less accurate this approach is.

Two different models for the rotation law were used. It is necessary to emphasize that the Brandt rotational curve is closer to real objects, but the calculations for it are more complex. However, the results do not have substantial differences (see Figures 1 and 2, Tables 3 and 6), so we can use the simpler model.

From a physical point of view, the parameter k_z is of primary importance. It can be shown that $1/k_z$ is the vertical lengthscale for the generated magnetic field, which has the same order as the thickness of the object (in dimensionless units). So, the possibility of such magnetic fields generation seems to be quite real and its lengthscales are comparable with the galaxy thickness. Nevertheless, we do not deny the possibility of other mechanisms producing magnetic fields, such as dynamo [25] or battery mechanisms [41].

Author Contributions: Conceptualization, E.M.; methodology, E.M.; investigation, T.K.; numerical results, T.K.; writing—original draft preparation, E.M. and T.K.; writing—review and editing, E.M. and T.K. All authors have read and agreed to the published version of the manuscript.

Funding: The research of E.M. was funded by the Russian Science Foundation, grant number 19-72-30028. The research of T.K. was funded by the Theoretical Physics and Mathematics Advancement Foundation «BASIS», project number #22-2-2-55-1.

Data Availability Statement: Data is contained within the article.

Conflicts of Interest: The authors declare no conflicts of interest.

References

1. Obridko, V.N.; Pipin, V.V.; Sokoloff, D.; Shibalova, A.S. Solar large-scale magnetic field and cycle patterns in solar dynamo. *Mon. Not. R. Astron. Soc.* **2021**, *504*, 4990–5000. [CrossRef]
2. Parker, E.N. Cosmical magnetic fields. Their origin and their activity. In *The International Series of Monographs on Physics*; Clarendon Press: Oxford, UK, 1979.
3. Glatzmaier, G.A.; Roberts, H. Rotation and Magnetism of Earth's Inner Core. *Science* **1996**, *274*, 1887–1891. [CrossRef]
4. Christensen, U.R. A deep dynamo generating Mercury's magnetic field. *Nature* **2006**, *444*, 1056–1058. [CrossRef]
5. Smith, E.J.; Davis, L., Jr.; Jones, D.E.; Coleman, J., Jr.; Colburn, D.S.; Dyal, P.; Sonett, C.; Frandsen, A.M.A. The planetary magnetic field and magnetosphere of Jupiter: Pioneer 10. *J. Geophys. Res.* **1974**, *79*, 3501. [CrossRef]
6. Borra, E.F.; Landstreet, J.D. The magnetic fields of the AP stars. *Astrophys. J. Suppl. Ser.* **1980**, *42*, 421–445. [CrossRef]
7. Vidotto, A.A.; Gregory, S.G.; Jardine, M.; Donati, J.F.; Petit, P.; Morin, J.; Folsom, C.P.; Bouvier, J.; Cameron, A.C.; Hussain, G.; et al. Stellar magnetism: Empirical trends with age and rotation. *Mon. Not. R. Astron. Soc.* **2014**, *441*, 2361–2374. [CrossRef]
8. Girart, J.M.; Rao, R.; Marrone, D. Magnetic Fields in the Formation of Sun-Like Stars. *Science* **2006**, *313*, 812–814. [CrossRef]
9. Moss, D.; Sokoloff, D.; Suleimanov, V. Dynamo generated magnetic configurations in accretion discs and the nature of quasi-periodic oscillations in accreting binary systems. *Astron. Astrophys.* **2016**, *588*, A18. [CrossRef]
10. Boneva, D.V.; Mikhailov, E.A.; Pashentseva, M.V.; Sokoloff, D.D. Magnetic fields in the accretion disks for various inner boundary conditions. *Astron. Astrophys.* **2021**, *652*, A38. [CrossRef]
11. Thompson, C.; Duncan, R.C. Neutron Star Dynamos and the Origins of Pulsar Magnetism. *Astrophys. J.* **1993**, *408*, 194. [CrossRef]
12. Moss, D. On the generation of bisymmetric magnetic field structures in spiral galaxies by tidal interactions. *Mothly Not. R. Astron. Soc.* **1995**, *275*, 191–194. [CrossRef]
13. Beck, R.; Brandenburg, A.; Moss, D.; Shukurov, A.; Sokoloff, D. Galactic Magnetism: Recent Developments and Perspectives. *Annu. Rev. Astron. Astrophys.* **1996**, *34*, 155. [CrossRef]
14. Berdyugina, S.V.; Solanki, S.K. The molecular Zeeman effect and diagnostics of solar and stellar magnetic fields. I. Theoretical spectral patterns in the Zeeman regime. *Astron. Astrophys.* **2002**, *385*, 701–715. [CrossRef]
15. Ginzburg, V.L. Radio astronomy and the origin of cosmic rays. *Paris Simp. Radio Astron. IAU Simp.* **1959**, *9*, 589. [CrossRef]
16. Han, J.L.; Manchester, R.N.; van Straten, W. Demorest, Pulsar Rotation Measures and Large-scale Magnetic Field Reversals in the Galactic Disk. *Astrophys. J. Suppl. Ser.* **2018**, *234*, 16. [CrossRef]
17. Manchester, R.N. Pulsar Rotation and Dispersion Measures and the Galactic Magnetic Field. *Astrophys. J.* **1972**, *172*, 43. [CrossRef]

18. Andreasyan, R.R.; Mikhailov, E.A.; Andreasyan, H.R. Structure and Features of the Galactic Magnetic-Field Reversals Formation. *Astron. Rep.* **2020**, *97*, 261. [CrossRef]
19. Kravchenko, E.; Giroletti, M.; Hada, K.; Meier, D.L.; Nakamura, M.; Park, J.; Walker, R.C. Linear polarization in the nucleus of M87 at 7 mm and 1.3 cm. *Astron. Astrophys.* **2002**, *637*, 9. [CrossRef]
20. Ro, H.; Kino, M.; Sohn, B.W.; Hada, K.; Park, J.; Nakamura, M.; Cui, Y. Spectral analysis of a parsec-scale jet in M 87: Observational constraint on the magnetic field strengths in the jet. *Astron. Astrophys.* **2023**, *673*, 16. [CrossRef]
21. Dormy, E.; Soward, A.M. *Mathematical Aspects of Natural Dynamos*; Chapman and Hall/CRC: New York, NY, USA, 2007.
22. Ruzmaikin, A.A.; Sokoloff, D.D.; Shukurov, A.M. *Magnetic Fields of Galaxies*; Springer: Berlin/Heidelberg, Germany, 1988; ISBN 90-277-2450-4.
23. Mikhailov, E.; Pashentseva, M. Eigenvalue Problem for a Reduced Dynamo Model in Thick Astrophysical Discs. *Mathematics* **2023**, *11*, 3106. [CrossRef]
24. Mikhailov, E.A. Symmetry of the magnetic fields in galactic dynamo and the material arms. *Magnetohydrodynamics* **2020**, *56*, 403.
25. Mikhailov, E.; Kasparova, A.; Moss, D.; Beck, R.; Sokoloff, D.; Zasov, A. Magnetic fields near the peripheries of galactic discs. *Astron. Astrophys.* **2014**, *568*, A66. [CrossRef]
26. Velikhov, E. Stability of an Ideally Conducting Liquid Flowing between Cylinders Rotating in a Magnetic Field. *Sov. J. Exp. Theor. Phys.* **1959**, *9*, 995–998.
27. Chandrasekhar, S. The Stability of Non-Dissipative Couette Flow in Hydromagnetics. *Proc. Natl. Acad. Sci. USA* **1960**, *46*, 253–257. [CrossRef] [PubMed]
28. Winters, W.F.; Balbus, S.A.; Hawley, J.F. Chaos in turbulence driven by the magnetorotational instability. *Mon. Not. R. Astron. Soc.* **2003**, *340*, 519–524. [CrossRef]
29. Balbus, S.A.; Hawley, J.F. Instability, turbulence, and enhanced transport in accretion disks. *Rev. Mod. Phys.* **1998**, *70*, 1–53. [CrossRef]
30. Korpi, M.J.; Mac Low, M.-M. A Numerical Investigation on the Role of the Magneto-rotational Instability in Galactic Disks. *Astron. Nachrichten* **2003**, *324*, 67.
31. Kitchatinov, L.L.; Rüdiger, G. Seed fields for galactic dynamos by the magnetorotational instability. *Astron. Astrophys.* **2004**, *424*, 565–570. [CrossRef]
32. Machida, M.; Nakamura, K.E.; Kudoh, T.; Akahori, T.; Sofue, Y.; Matsumoto, R. Dynamo Activities Driven by Magnetorotational Instability and the Parker Instability in Galactic Gaseous Disks. *Astrophys. J.* **2013**, *764*, 9. [CrossRef]
33. Shakura, N.I.; Postnov, K.A.; Kolesnikov, D.A.; Lipunova, G.V. Magnetorotational instability in Keplerian disks: A nonlocal approach. *Phys. Uspekhi* **2023**, *66*, 1262–1276. [CrossRef]
34. Shakura, N.I.; Sunyaev, R.A. Black holes in binary systems. Observational appearance. *Astron. Astrophys.* **1973**, *24*, 337–355.
35. Brandt, J.C. On the Distribution of mass in Galaxies. I. The Large-Scale Structure of Ordinary Spirals with Applications to M 31. *Astrophys. J.* **1960**, *131*, 293. [CrossRef]
36. Yoshiaki, S. The Most Completely Sampled Rotation Curves for Galaxies. *Astrophys. J.* **1996**, *458*, 120.
37. De Block, W.J.G.; Walter, F.; Brinks, E.; Trachternach, C.; Oh, S.H.; Kennicutt, R.C., Jr. Hight-resolution Rotation Curves and Galaxy Mass Models from Things. *Astron. J.* **2008**, *136*, 2648. [CrossRef]
38. Roberts, M.S.; Whitehurst, R.N. The rotation curve and geometry of M31 at large galactocentric distances. *Astrophys. J.* **1975**, *201*, 327–346. [CrossRef]
39. Landau, L.D.; Lifshitz, E.M. Theoretical physics. In *Quantum Mechanics (Non-Relativistic Theory)*; Pergamon Press: Oxford, UK, 1977.
40. Khasaeva, T.T.; Mikhailov, E.A. Mehanismy formirovaniya magnitnyh poley na bolshom rasstoyaniy ot centra galaktiki. *Zhurnal Teh. Fiz.* **2023**, *93*, 1771.
41. Andreasyan, R.R. Mechanism of formation of a dipole magnetic field in the central regions of active galaxies. *Astrophysics* **1996**, *39*, 58–62. [CrossRef]